Pis'ma v ZhETF, vol. 92, iss. 1, pp. 59 – 64

Temperature dependence of radiative recombination in CdSe quantum dots with enhanced confinement

S. V. Zaitsev[1)], *T. Kümmell*[*], *G. Bacher*[*], *D. Hommel*[+]

Institute of Solid State Physics RAS, 142432 Chernogolovka, Russia

[*] *Universität Duisburg-Essen, 47057 Duisburg, Germany*

[+] *Institut für Festkörperphysik, Halbleiterepitaxie, Universität Bremen, 28359 Bremen, Germany*

Submitted 11 May 2010

Resubmitted 25 May 2010

We studied in details the recombination dynamics and its temperature dependence in epitaxially grown neutral CdSe/ZnSSe quantum dots with additional wide-band gap MgS barriers. Such design allows to preserve a very high quantum yield and track the radiative recombination dynamics up to room temperature. A fast initial decay of ~ 0.6 ns followed by a slow decay with a time constant $\sim 30 - 50$ ns is observed at low temperature $T < 50$ K. The fast decay gradually disappears with increasing temperature while the slow decay shortens and above 100 K predominantly a single-exponential decay is observed with a time constant ~ 1.3 ns, which is weekly temperature dependent up to 300 K. To explain the experimental findings, a two-level model which includes bright and dark exciton states and a temperature dependent spin-flip between them is considered. According to the model, it is a thermal activation of the dark exciton to the bright state and its consequent radiative recombination that results in the long decay tail at low temperature. The doubling of the decay time at high temperatures manifests a thermal equilibrium between the dark and bright excitons.

Self-assembled quantum dots (QDs) in semiconductor heterostructures are of great fundamental interest because of their discrete atom-like energy levels and promising optical properties both for QD lasers and quantum information applications [1, 2]. The discrete energy level structure of QDs triggered a variety of innovative optoelectronic applications like a single photon source [3, 4]. For device operation at ambient conditions a detailed understanding of the radiative recombination dynamics and its evolution with temperature is required. However, non-radiative losses as well as thermal emission to the barriers prevented the study of the radiative recombination dynamics in self-assembled quantum dots up to room temperature until now [5, 6].

Theoretically, due to intrinsic disorder and/or a finite localization of excitons, the exciton oscillator strength in quasi-two-dimentinal quantum well structures decreases significantly giving rise to the exciton lifetimes τ of the order of several hundreds picosecond (ps) [7] as observed experimentally [8]. Further increase of exciton localization in self-organized QDs where a full spatial confinement takes place results in a growth of τ up to 0.5 nanosecond (ns) in self-organized CdSe QDs [9, 5] and 1-2 ns in InAs/GaAs [10, 11], which is consistent with calculations [12, 13].

An electron-hole exchange interaction, which is strongly increased by the spatial confinement in QDs, splits exciton states in neutral QDs [14]. The ground energy state has a total angular momentum projection $m = \pm 2$ and thus it is optically inactive while the next excited state with $m = \pm 1$ is electric-dipole allowed and, therefore, these levels are usually referred to as "dark" and "bright" exciton states [15]. An energy splitting $\triangle E$ between dark and bright states depends on the QD radius and typically amounts to 1.5-2 meV in self-assembled CdSe QDs [16].

In time-resolved studies of QDs, a fast, almost mono-exponential decay, with the decay time ~ 1 ns or less usually takes place at low temperature in InAs/GaAs or CdSe QDs [9, 11, 17]. Surprisingly, a long-decay component within ns-time domain was observed, e.g., in InP/GaInP QDs [18], InGaAs/GaAs [19] or in CdSe self-assembled QDs [20, 21]. This slow tale was attributed either to localized carriers in the tail states below band edges in the disordered GaInP matrix [18], to some specific electronic states of the QDs [20] or to a lateral carrier migration within the complex $Cd_xZn_{1-x}Se$ landscape formed in a thin QDs layer with a nominal CdSe composition [21]. Another explanation was proposed by Smith et al. who suggested that the dark excitons contribute to the signal by undergoing a spin flip to the bright state and decaying radiatively [19].

[1)] e-mail: szaitsev@issp.ac.ru

Here we present investigations of the time-resolved photoluminescence (PL) emission and its dynamics in ensemble of epitaxially grown neutral CdSe/Zn(S,Se) QDs, sandwiched between additional thin MgS barriers. This design allows to preserve a very high quantum yield and track the QDs recombination dynamics up to room temperature. We find that the bright-dark exciton two-level model gives qualitative and quantitative description of the recombination dynamics and its temperature dependence in the ps- and ns-time domains.

The investigated self-assembled CdSe QDs with enhanced confinement (sample A) were grown by a migration enhanced epitaxy on a i-GaAs substrate with a 50-nm-thick ZnSe buffer [22] and embedded into a specially designed symmetric barriers. The barriers consist of 1.4 nm thick $ZnS_{0.4}Se_{0.6}$ layers for increasing the lateral carrier confinement followed by MgS layers of $\sim$ 1.0 nm thickness (inset in Fig. 1), which provide a high confinement for both electrons and holes in vertical (growth) direction. For investigated sample the MgS barriers have been chosen since this material has one of the highest bandgaps available in the II-VI system ($E_g \approx 5.5$ eV). Finally, this structure was capped by a ZnSe layer of 25 nm. Such design allows to preserve a very high quantum yield and study parameters of a single QD emission up to 300 K [23]. A reference structure (sample B) with a typical design of CdSe QDs layer and ZnSe barriers was also grown in a similar way. A QDs density was $\sim 5 \cdot 10^{10}$ cm^{-2} as observed by a high resolution scanning electron microscopy which allows to exclude a direct inter-QDs coupling.

The ps-time-resolution measurements were carried out in a closed cycle helium cryostat providing a temperature range of 5-300 K with a sample fixed on the cooled finger. Setup includes a Ti:Sa picosecond laser with a frequency doubler (76 MHz, $\lambda_{exc} = 400-450$ nm), a monochromator with a spectral resolution better than 1 meV, and a streak camera with a time resolution of 8 ps. The average power density of the exciting laser was $P_L \sim 50$ W/cm^2, which allowed to eliminate the many-particle effects and overheating of samples. In the ns-time domain studies a pulsed diode laser ($\lambda_{\text{exc}} = 405$ nm, $P_L \sim 0.5$ W/cm^2) with a repetition rate of 1–80 MHz and a time-correlated single photon counting system using a microchannel plate multiplier was applied for detection. Overall time resolution in these measurements is $\sim$ 80 ps.

The temporal decays of a spectrally integrated QDs PL intensity in the temperature range 5-296 K, measured with the streak camera, are shown for both samples in Fig.1. A rise time after the laser pulse is less than 20 ps which reflects rather fast initial relaxation process into

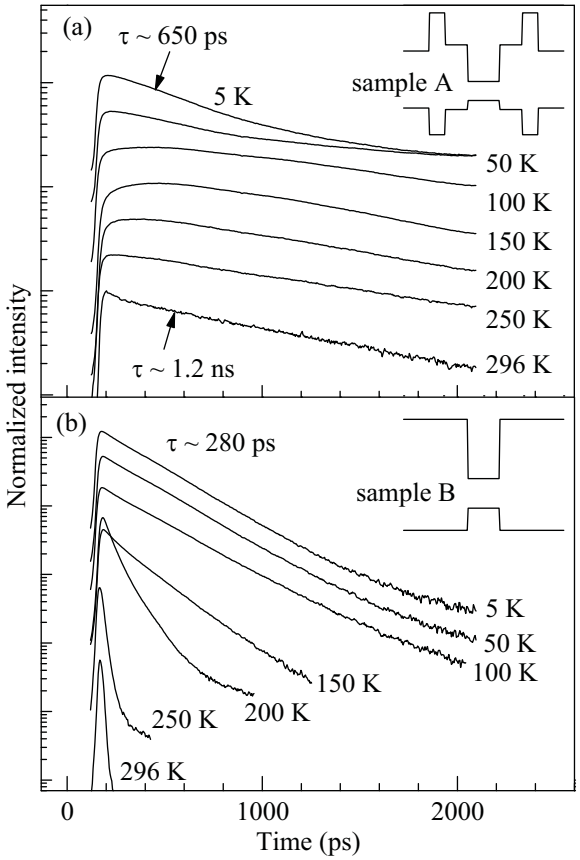

Fig.1. The PL decays vs temperature in the ps-time domain for sample A (a) and sample B (b) at $P_L \sim 50$ W/cm^2 and $\lambda_{exc} = 400$ nm. Insets show corresponding QDs band alignment

the QD ground state. One can see that in sample B the decays shorten significantly at $T > 100$ K (Fig.1b) which reflects increasing non-radiative losses at elevated temperatures partly by a straightforward recombination with a tunneling close non-radiative centers or due to temperature induced escape to the nearby barriers or wetting layer [24]. This conclusion is also supported by the temperature dependence of time-integrated intensity which drops almost tree orders of magnitude at $T = 300$ K as compare to cryogenic temperatures (Fig.2). On the other hand, in sample A the intensity decreases only 10-40 times, depending on the excitation ps-laser λ_{exc} and P_L. Thus, this result directly shows a suppression of the non-radiative recombination in the case of enhanced spacial confinement of QDs.

In sample A the decay curves at low temperatures $T < 100$ K are not mono-exponential but rather have fast and slow components of $\sim$ 0.65 ns and $\sim$ 30 ns, respectively, which is clearly seen from the ns-time range measurements (Fig.3a). We note that the low temperatures decays cannot be fitted well by a two-exponential

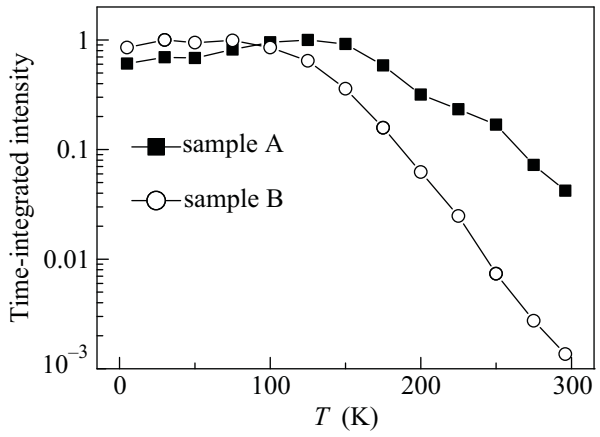

Fig.2. The dependencies of the time-integrated intensity vs temperature for both samples at $P_L \sim 50\,\mathrm{W/cm^2}$ and $\lambda_{exc} = 400\,\mathrm{nm}$

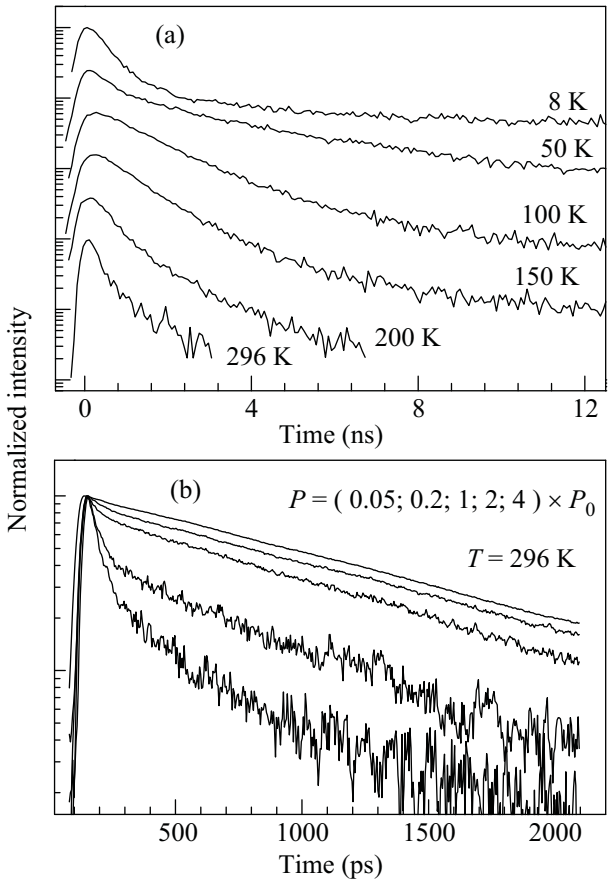

Fig.3. (a) The PL decays vs temperature in the ns-time domain for sample A at $P \sim 0.5\,\mathrm{W/cm^2}$. (b) The excitation power dependence of decays for sample A at room temperature ($P_0 = 50\,\mathrm{W/cm^2}$ and $\lambda_{exc} = 455\,\mathrm{nm}$)

but rather by a stretched-exponential dependence, which reflects an inhomogeneous distribution of the slow recombination times in the ensemble of QDs, as supported by a broad spectrum of the QDs ensemble of $\sim 70 - 80\,\mathrm{meV}$. The nature of the slow component will be discussed in details later. In the ps-domain measurements the initial fast decay part disappears at $T \sim 100\,\mathrm{K}$ and a slower, nearly mono-exponential decay remains (Fig.1a). Simultaneously, a delay of ~ 0.5 ns between the laser pulse and intensity maximum is formed, which looks like a plateau in the decay curve and is observed up to 200 K. Such a plateau in decay correlates with some increase of intensity (~ 1.5 times) in sample A in this temperature range (Fig.2). We suppose that both experimental findings can be explained by a thermal excitation to the wetting layer of electrons or holes, separately captured into QDs, their redistribution in the QD ensemble and eventual radiative recombination at elevated temperatures, similar to results of Ref. [24].

Above 250 K, in the ps-time-domain studies only a single-exponential decay dominates with the decay time of $\sim 1.2 - 1.3\,\mathrm{ns}$ (Fig.1a), which is slightly dependent on the wavelength of excitation laser. Similar behavior is observed in the ns-studies only up to $T \sim 150\,\mathrm{K}$ (Fig.3a) while at higher temperature a gradual decrease of the decay time and PL intensity takes place, as compare to ps-excitation. Such a difference is explained by a rather low excitation laser power density, available in this studies (maximum $P \sim 0.5\,\mathrm{W/cm^2}$). This fact is directly confirmed by the power dependence of decays at ps-excitation laser, presented in Fig.3b. It is seen that the fast initial non-radiative decay disappears with increasing of P and a long tale with $\tau \sim 1.3\,\mathrm{ns}$ is established at high power density which is typical for saturation of the non-radiative recombination channel with increasing carrier density.

One should more clearly explain a physical picture behind the experimental data for sample A. On one side we observed a decrease of the QDs intensity at high $T > 150\,\mathrm{K}$ (Fig.2). On the other side the lifetime in this temperature range changes only slightly which looks like a contradiction with the behavior of the QDs intensity. To understand such a difference, we need to recall that at non-resonant photoexcitation of QDs, used in our studies, the electron-hole pairs are created mostly in the nearby barrier or wetting layers and then carriers are captured into QDs [24]. Thus, the only possibility to explain both experimental findings is to assume that the main non-radiative losses occur in the barrier or wetting layers, before the carriers are captured to QDs. From Fig.2 one can conclude that the effective non-radiative recombination in these layers starts above 150 K. It is important to note that a radiative recombination of the barrier or wetting layers has not been observed in investigated samples which means that another processes

are much faster. As to the carriers relaxed to QDs, the non-radiative channels inside QDs are really very weak and can be saturated easily even at room temperature and under photoexcitation below the ZnSSe barrier, i.e., to the wetting layer only (Fig.3b).

Generally, in self-assembled QDs an almost mono-exponential decay is observed with $\tau = 0.3-1.2$ ns which is considered as an exciton radiative recombination lifetime τ_b of the bright exciton [9, 11, 17]. The spin-flip of bright excitons to dark ones in such QDs is strongly reduced at low temperature, with a typical values of a spin-flip time $\tau_{sf} \sim 5 - 10$ ns [25], much longer than τ_b. So, its influence on the PL decay should not be significant at low temperature. However, the detailed studies of the single CdSe QDs revealed a substantial impact of the dark exciton state on the PL transients [5, 19]. It was suggested that a thermally activated population of the bright exciton state from the energetically lowest dark state gives rise to the slow component in the decay of neutral QD. Interestingly, the decay dynamics of the trion is strictly mono-exponential in accordance with the absence of dark states for trion, thus confirming the suggestion [5]. Theoretical analysis have shown that a thermal equilibrium between the bright and dark excitons significantly changes the decay dynamics also at high temperatures [13]. What is important, an apparent decay time τ tends to twice of τ_b ($\tau \to 2\tau_b$) in conditions when $\tau_b \gg \tau_{sf}$, which is realized at high temperatures. These predictions have not been confirmed up to now because of the high non-radiative losses in self-organized QDs [5, 6].

The PL efficiency at room temperature in the presented QD system with enhanced confinement is improved significantly which allowed us to check the conclusions of Ref. [13]. In our consideration we base on a two-level energy scheme for bright-dark excitons system, i.e., assuming predominantly neutral QD in the studied samples. This assumption is strongly supported, on one side, by a mono-exponential decay dynamics for the charged excitons (trion) in single QDs [5]. On the other side, in controlled growth conditions with increasing Cl content in the ZnSSe layer a gradual change of the decay dynamics and its temperature dependence from the two-exponential to the mono-exponential decay takes place at low temperatures. Cl is usually used as n-type dopant in ZnSSe [22] and would lead to increasing of the single-charged QDs, thus confirming our assumption about major neutrality of QDs in our sample without intentional doping.

The considered two-level model (inset in Fig.2a) corresponds to the dark and bright exciton states with the latter being higher in energy [14]. A system of coupled differential equations for population probability of dark ($n_d(t)$) and a bright state ($n_b(t)$) can be written as [5, 19]:

$$dn_b/dt = -n_b(1/\tau_b + 1/\tau_{sf} + 1/\tau_{nr}) + n_d/\tau'_{sf}, \quad (1)$$

$$dn_d/dt = -n_d(1/\tau_d + 1/\tau'_{sf} + 1/\tau_{nr}) + n_b/\tau_{sf}, \quad (2)$$

where τ_{sf} and τ'_{sf} are the spin-flip time of bright exciton to dark and vice versa, τ_d – a radiative recombination lifetime of dark exciton and τ_{nr} is a non-radiative recombination lifetime. Usually direct recombination of the dark exciton can be ruled out by symmetry considerations [26] due to absence of admixture between dark and bright states: $\tau_d \to \infty$. In the following calculations we put $\tau_d = 1$ ms. As to the τ_{sf} and τ'_{sf}, we adopt the model of acoustic phonons assisted spin-flip which was recently shown to be the main mechanism in NCs [27]. In self-organized QDs there is a continuum of acoustic modes related to the host semiconductor with nearly similar elastic parameters as of the QDs, making this mechanism very feasible also. Indeed, theoretical consideration and calculations have confirmed high efficiency of acoustic phonons for spin-flip between bright and dark states through the combined action of short-range exchange interaction and Bir-Pikus deformation potential terms which results in τ_{sf} comparable to τ_b already at temperatures of several tens kelvins [28]. This model assumes a strong temperature dependence of τ_{sf} and τ'_{sf} due to a Bose-factor $n_B(T) = 1/(\exp(\triangle E/kT) - 1)$:

$$1/\tau_{sf} = [n_B(T) + 1]/\tau_{sf,o}\ , \quad 1/\tau'_{sf} = n_B(T)/\tau_{sf,o}, \quad (3)$$

where $\triangle E$ – is a dark-bright splitting.

At non-resonant excitation of QDs with a random spin distribution of photoexcited carriers the initial values of the population probabilities for dark and bright states are equal: $n_d(0) = n_b(0) = 1/2$. The results of calculations are shown in Fig.4 for $\triangle E = 2$ meV, $\tau_b = 0.65$ ns (fast decay time at low T), $\tau_{sf,o} = 5$ ns (Ref. [25]), $\tau_d = 1$ ms and $\tau_{nr} \to \infty$. The last assumption means that we neglect the non-radiative losses which can be saturated even at room temperature at moderate laser power in the studied QDs with enhanced confinement (Fig.3b).

One can see that calculations reproduce very well the temperature change of the measured decay curves (Fig.1a). At low temperatures the calculated decays show fast and slow components of ~ 0.6 ns and ~ 100 ns which correspond to decays of the bright and dark excitons, respectively. As follows from analysis of equa-

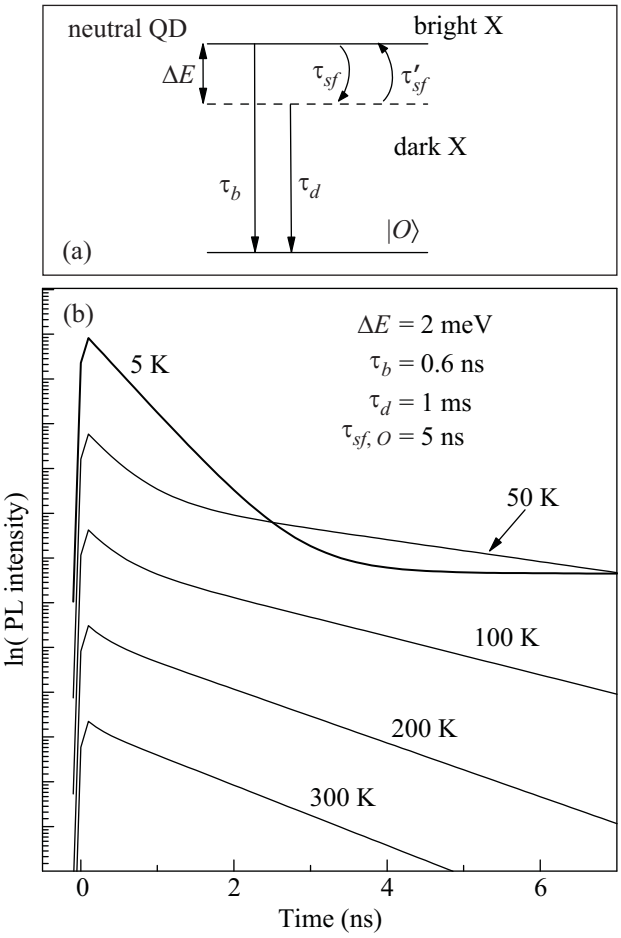

Fig.4. (a) The scheme of two-level model with corresponding transitions (see text). (b) Results of the model calculations: decays at different T with a set of parameters depicted in figure. Decays are shifted for clarity

tions (1-2), the slow time roughly equals to $\tau'_{sf} \propto$ $\propto \exp(\triangle E/kT)$ at low T and this component describes the decay of dark excitons by their thermal excitation to the bright states. Such a strong, exponential dependence of τ'_{sf} vs $\triangle E$ explains the mentioned above fact that the experimental decays cannot be fitted satisfactorily by simple two-exponential curves in conditions of inhomogeneous distribution of $\triangle E$ in the QDs ensemble. Above 100 K the fast component almost disappears while the slow component gradually gets stronger and faster, finally achieving ~ 1.45 ns at $T = 300$ K. This is in accordance with the analysis given in Ref. [13] and just reflects an establishing of the thermal equilibrium between the dark and bright excitons at high temperature, thus giving rice to approaching of "apparent" decay time τ to the doubled τ_b.

It is known from mathematics that a solution of the linear system of ordinary differential equation like (1-2) with constant coefficients is a sum of two exponents with the characteristic decay times $\tau_{1,2}$ and amplitudes $A_{1,2}$ which are determined by the coefficients and initial conditions, respectively [29]. We identify these two exponents with the fast and slow characteristic decays observed in experiment. The results of calculated in this way $\tau_{1,2}$ and amplitudes $A_{1,2}$ are shown in Fig.5 together with the decay times τ determined from experiment (Figs.1a and 3a). One can see that at low $T < 50$ K the experimental decay times obtained from the slope of the decay curves in the ps-time domain are closer to the calculated fast decay time τ_1. At high $T > 50$ K they fit better to the calculated slow time τ_2. Similar results are observed also in the ns-time domain: fitted values of $\tau_{1,2}$ correspond very well to calculated ones at $T = 5 - 50$ K. At higher temperatures $\sim 70 - 150$ K only the first component can be reliably determined from the fit. The fitted value of τ_1 in this case better corresponds to the calculated slow time τ_2.

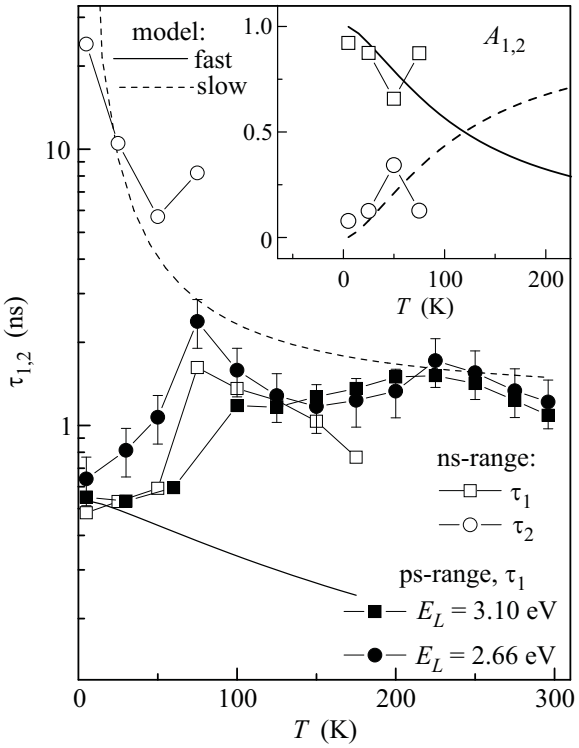

Fig.5. The calculated model decay times $\tau_{1,2}$ and amplitudes $A_{1,2}$ vs T. Parameters used for calculations are the same as in Fig.4. Symbols present the decay times τ determined from fit of experimental decays in different conditions (marked in figure)

Such a strange at first glance situation can be understood by accounting of the relative magnitudes of both components (inset in Fig.5). According to calculations, for chosen set of parameters, at low $T < 100$ K domi-

nates the fast component while at high $T > 100\,\mathrm{K}$ – the slow one. In conditions of the mentioned above large inhomogeneous distribution of the QDs parameters the reliable fit is not possible in intermediate $T \sim 100\,\mathrm{K}$ where a "jump" from one branch to another takes place. Note that exactly this situation in decay dynamics was predicted theoretically by Narvaez et al. [13].

In conclusion we summarize the results of our studies of temperature dependent recombination dynamics in the high quality self-assembled CdSe/Zn(S,Se)/MgS QDs. The improved barrier design allowed to achieve a very high quantum yield and track the PL decay dynamics up to room temperature. Thus we were able to check experimentally the predictions of the two-level model for the recombination dynamics in neutral QDs. We found that the two-level model satisfactorily describes the recombination dynamics of the neutral QDs. The decay curves at low temperatures ($< 100\,\mathrm{K}$) contain both fast and slow parts with characteristic times, corresponding to the decays of bright and dark excitons, respectively. The slow component describes the decay of dark excitons by their thermal activation to the bright states. Increasing of temperature gives rise to dominance of the slow component with the simultaneous decrease of its decay time value to that roughly twice of the fast decay time at low T. The analysis of the rate equations in frames of two-level model shows that such an increase (~ 2 times) of the apparent decay time corresponds to establishing of thermal equilibrium between the dark and bright excitons at high temperature.

This work is partly supported by grant # 09-02-00770 of Russian Foundation for Basic Research and grant SFB # 445.

1. D. Bimberg, M. Grundmann, and N. N. Ledentsov, *Quantum Dot Heterostructures*, Wiley and Sons, New York, 1999.
2. A. J. Shields, Nature Phot. **1**, 215 (2007).
3. Z. Yuan, B. E. Kardynal, R. M. Stevenson et al., Science **295**, 102 (2002).
4. M. Scholz, S. Büttner, O. Benson et al., Opt. Express **15**, 9107 (2007).
5. B. Patton, W. Langbein, and U. Woggon, Phys. Rev. B **68**, 125316 (2003).
6. P. Bajracharya, T. A. Nguyen, S. Mackowski et al., Phys. Rev. B **75**, 035321 (2007).
7. D. S. Citrin, Phys. Rev. B **47**, 3832 (1993).
8. H. Yu, C. Roberts, and R. Murray, Phys. Rev. B **52**, 1493 (1995).
9. T. Kümmell, R. Weigand, G. Bacher et al., Appl. Phys. Lett. **73**, 3105 (1998).
10. G. Wang, S. Fafard, D. Leonard et al., Appl. Phys. Lett. **64**, 2815 (1994).
11. A. Fiore, P. Borri, W. Langbein et al., Appl. Phys. Lett. **76**, 3430 (2000).
12. D. S. Citrin, Superlattices Microstruct. **13**, 303 (1993).
13. G. A. Narvaez, G. Bester, A. Franceschetti et al., Phys. Rev. B **74**, 205422 (2006).
14. V. D. Kulakovskii, G. Bacher, R. Weigand et al., Phys. Rev. Lett. **82**, 1780 (1999).
15. Al. L. Efros, M. Rosen, M. Kuno et al., Phys. Rev. B **54**, 4843 (1996).
16. E. A. Chekhovich, A. S. Brichkin, A. V. Chernenko et al., Phys. Rev. B **76**, 165305 (2007).
17. G. Bacher, R. Weigand, J. Seufert et al., Phys. Rev. Lett. **83**, 4417 (1999).
18. T. Okuno, Hong-Wen Ren, M. Sugisaki et al., Phys. Rev. B **15**, 1386 (1998).
19. J. M. Smith, P. A. Dalgarno, R. J. Warburton et al., Phys. Rev. Lett. **94**, 197402 (2005).
20. L. M. Robinson, H. Rho, J. C. Kim et al., Phys. Rev. Lett. **83**, 2797 (1999).
21. S. Rodt, V. Türck, R. Heitz et al., Phys. Rev. B **67**, 235327 (2003).
22. A. Gust, C. Kruse, and D. Hommel, J. Cryst. Growth **301**, 789 (2007).
23. R. Arians, T. Kummell, G. Bacher et al., Appl. Phys. Lett. **90**, 101114 (2007).
24. A. Polimeni, A. Patane, M. Henini et al., Phys. Rev. B **59**, 5064 (1999).
25. V. D. Kulakovskii, R. Weigand, G. Bacher et al., phys. Stat. Sol. (a) **178**, 323 (2000).
26. B. Urbaszek, R. J. Warburton, K. Karrai et al., Phys. Rev. Lett. **90**, 247403 (2003).
27. D. Oron, A. Aharoni, Celso de Mello Donega et al., Phys. Rev. Lett. **102**, 177402 (2009).
28. K. Roszak, V. M. Axt, T. Kuhn et al., Phys. Rev. B **76**, 195324 (2007).
29. See, e.g., web-cite http://www.efunda.com/math/ode/syslinearode1.cfm.